COMPARISON OF TWO MODELS OF NUMERICAL SIMULATION OF LOW CYCLE FATIGUE OF A PLASTIC MATERIAL WITH SMALL RIGID INCLUSIONS

JOURY M. TEMIS, KHAKIM KH. AZMETOV

Central Institute of Aviation Motors, Moscow, Russia

e-mail: tejoum@ciam.ru

WILLIAM J. FLEMING

Northumbria University, School of Computing, Engineering and Information Sciences, Newcastle upon Tyne, U.K.

Theory of Cells and a numerical FE method based on strain cyclic plasticity, damage model and technology of died elements were used for a prediction of the fatigue life of a metal matrix composite material. Results of calculations were compared with experimental fatigue data. It was shown that the predicted fatigue life of MMC using the method of cells was in close agreement with the experimental results for life outside of low cycle fatigue regime of 1000 cycles or less. The results obtained from the mathematical simulation procedure show that the failure occurs in several steps – the process of damage accumulation in the material and the process of crack growth. The results of prediction of time of the composite material full fracture are in good agreement with experimental data. The comparison shows that both the numerical method and the theory of cells can be used to predict fatigue life of MMC to within an acceptable degree of accuracy.

Key words: low cycle fatigue, cyclic plasticity, damage accumulation model

1. Introduction

The introduction of inclusions into a base metal will give greatly enhanced mechanical properties to the resultant metal matrix composite (MMC). However, these properties will depend on the properties of both the base matrix and the inclusions used. The inclusion volume ratio and its geometrical form will, of course, also be important. These parameters and the parameters of the interface between the matrix and inclusion define both the composite ultimate strength under monotonic loading and fatigue strength under cyclic loading. The main problem facing the material designer is to create composite materials or a structure with superior mechanical properties. To solve this problem, experimental research is mainly employed. This method is expensive and it does not allow an easy optimisation of the material or component properties.

A mathematical approach would appear to offer a more economical methodology of selecting likely candidate composite materials and thus limiting the amount of experimentation necessary to produce successful materials. In this study, two mathematical approaches are used, one analytical using the Theory of Cells (Fleming and Dowson, 1999) and the other, a numerical method using based on a cyclic plasticity and accumulated plasticity strain damage models and a finite element approach for cycling loading (Temis, 1989, 1994; Putchkov *et al.*, 1995). The methods were used to predict the fatigue life of a metal matrix composite over a range of strain values, and then the predicted results were compared to experimental results.

2. Experimental testing

2.1. Material

The materials under consideration in this report are an aluminium alloy Al7075 and a metal matrix composite with an identical material for the matrix plus 12% SiC fibres, in particulate form. The chemical composition of the composite was 6.2% Zn, 1.5% Cu, 2.3% Mg, 0.2% Cr, 0.3% Fe and the remainder aluminium. The monolithic material had a Young's modulus of 72 GPa, a Poisson's ratio 0.33, a 0.2% proof stress of 416 MPa, a UTS of 565 MPa and an elongation at failure of 14%.

The SiC particles had the following specification. Diameters range from 0.25 to 20 microns with an average diameter of 3 microns to 4 microns. The average effective aspect ratio was 1.3 whilst the Young's modulus was 468 GPa and the Poisson's ratio was 0.25. The particulate strength was assumed to be statistical in nature, 5% of the particulates failing at a stress of 1.6 GPa and 90% having failed at an average stress of 3.1 GPa.

The MMC's were produced by spray forming followed by extrusion. Heat treatment of the material consisted of an initial high temperature solution treatment at 465°C held for 45 minutes followed by a cold-water quench and the material aged for 16hr at 135°C. The measured Young's modulus was then 84 GPa, the 0.2% proof stress 404 MPa, the UTS 490 MPa and its elongation at failure was 2%.

2.2. Testing Procedure

The tests were carried out on a PC driven 50 kN capacity Dartec servo-hydraulic testing machine. All tests were conducted under strain control and constant amplitude. The tests were conducted in air at a frequency of 0.25 Hz using fully reversed loading $(R = -1.0)$ with stress and strain data being recorded for each cycle.

2.3. Results

The tests were carried out on both the monolithic and metal matrix material at a constant strain rate with the stress being allowed to vary (Fig. 1). In both cases, for the low strain rates, the stress was fairly constant throughout each individual experiment. However, once the material was strained into the plastic region, work hardening took place and therefore the stress increased throughout the life of the test (Fleming and Dowson, 1999).
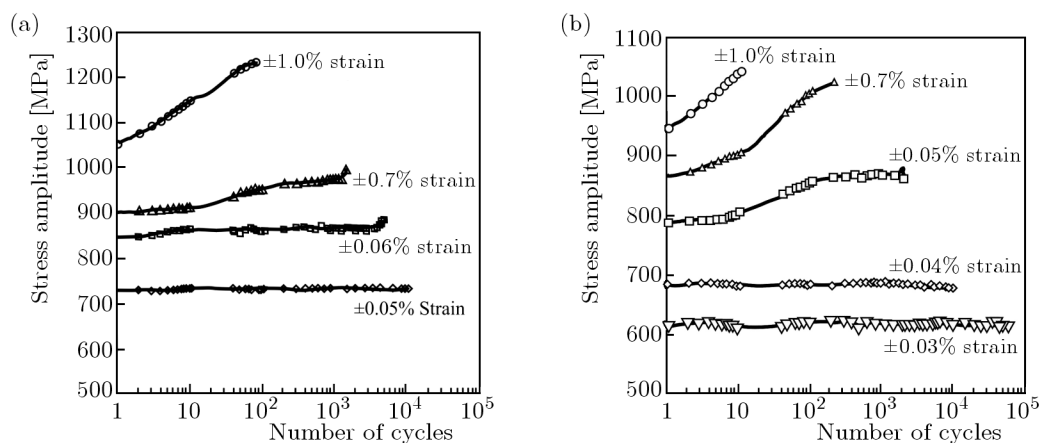

Fig. 1. Strain controlled fatigue test on monolithic Al7075 (a) and on Al7075/12% SiC (b)

3. Theory

3.1. Theory of Cells

The Theory of Cells (TOC) for short fibre and particulate metal matrix composites has been developed by Aboudi (1991). In the method, an elastic matrix is considered whose unidirectional fibres of short length reinforce it. The fibres are assumed rectangular with dimensions of d_1, l_1 and h_1 and arranged in the matrix as shown in Fig. 2a. In a particulate metal matrix composite, h_1 will have a similar value to l_1.

Given that the arrangement of fibre and matrix are periodic, only one fibre and its surround matrix need be analysed to give a representative section of the composite material (Fleming and Dowson, 1999). This area is called a cell and is shown in Fig. 2b.
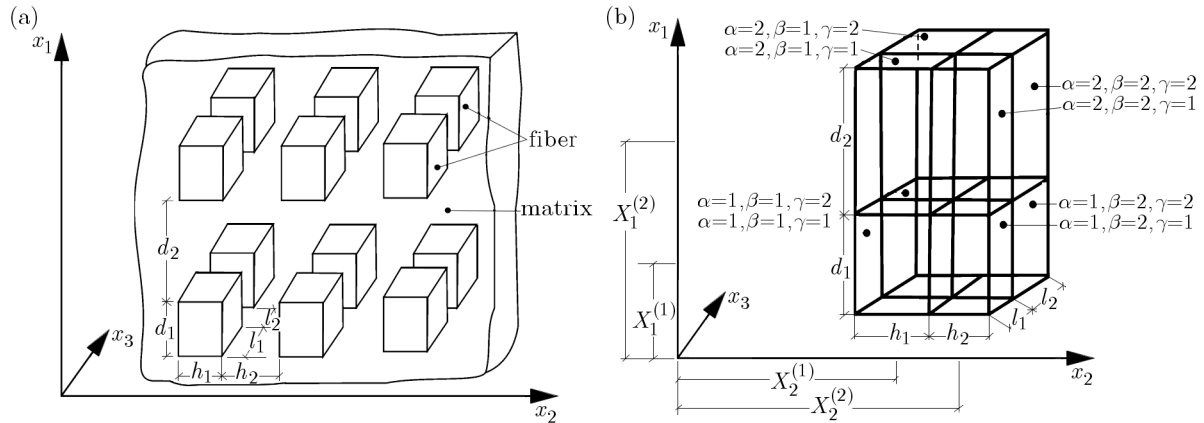

Fig. 2. (a) Schematic of an MMC with a periodic array of fibres; (b) a representative cell of the composite showing the eight sub-cells

As can be seen, each cell comprises eight sub-cells, one of fibre, labelled 1,1,1, and seven of the matrix material. It is assumed, initially, that both fibres and matrix are perfectly elastic materials, and the stresses are related to the strains as follows

$$\boldsymbol{\sigma}^{(\alpha,\beta,\gamma)} = \mathbf{C}^{(\alpha\beta\gamma)}\mathbf{Z}^{(\alpha\beta\gamma)} - \boldsymbol{\Gamma}^{(\alpha\beta\gamma)}\Delta T \tag{3.1}$$

where: $\boldsymbol{\sigma}^{\alpha,\beta,\gamma}$ is the stress matrix of each sub-cell; $\mathbf{C}^{\alpha\beta\gamma}$ – stiffness matrix representing mechanical properties of each sub-cell; $\boldsymbol{\Gamma}^{\alpha\beta\gamma}$ – matrix representing thermal properties of each sub-cell; ΔT – temperature difference between the reference stress free temperature and the working temperature; whilst $\mathbf{Z}$, the strain microvariables, is given by

$$\mathbf{Z}^{(\alpha\beta\gamma)} = [\Phi_1^{(\alpha\beta\gamma)}, X_2^{(\alpha\beta\gamma)}, \Psi_3^{(\alpha\beta\gamma)}, X_1^{(\alpha\beta\gamma)} + \Phi_2^{(\alpha\beta\gamma)}, \Psi_1^{(\alpha\beta\gamma)} - \Phi_3^{(\alpha\beta\gamma)}, \Psi_2^{(\alpha\beta\gamma)} + X_3^{(\alpha\beta\gamma)}] \tag{3.2}$$

with $\Phi_1^{(\alpha\beta\gamma)}, \Phi_2^{(\alpha\beta\gamma)}, \Phi_3^{(\alpha\beta\gamma)}, X_1^{(\alpha\beta\gamma)}, X_2^{(\alpha\beta\gamma)}, X_3^{(\alpha\beta\gamma)}, \Psi_1^{(\alpha\beta\gamma)}, \Psi_2^{(\alpha\beta\gamma)}, \Psi_3^{(\alpha\beta\gamma)}$ – representing strain microvariables.

Note that when discussing the position of a sub-cell, a superscript notation is used, i.e., $\boldsymbol{\sigma}^{(1,1,1)}$ refers to the fibre whilst, for instance, $\boldsymbol{\sigma}^{(1,2,1)}$ is the matrix material to the right of the fibre, and subscript notation is used for the stress direction, e.g. σ_{11} for the direct stress in the x_1 direction.

Using a first order approximation, the displacement component at any point in the sub-cell can be expressed as

$$u_i^{(\alpha\beta\gamma)} = w_i^{(\alpha\beta\gamma)} + x_1^{(\alpha)}\Phi_i^{(\alpha\beta\gamma)} + x_2^{(\beta)} + X_i^{(\alpha\beta\gamma)} + x_3^{(\gamma)}\Psi_i^{(\alpha\beta\gamma)} \tag{3.3}$$

where w_i represents the displacement component of the centre of the sub cell and Φ_i, X_i, Ψ_i characterises the linear dependence of the displacements on the local co-ordinates $x_1^{(\alpha)}$, $x_2^{(\beta)}$, $x_3^{(\gamma)}$, and the displacement can be connected to strain using the expression

$$\varepsilon_{ij}^{(\alpha,\beta,\gamma)} = \frac{1}{2}\left[\partial_j u_i^{(\alpha\beta\gamma)} + \partial_i u_j^{(\alpha\beta\gamma)}\right] \tag{3.4}$$

where $\partial_1 = \partial/\partial x_1^\alpha$, $\partial_2 = \partial\partial x_2^\beta$, $\partial_3 = \partial/\partial x_3^\gamma$.

If the continuity of traction and displacement between appropriate sub-cells is assumed, it is possible to calculate 26 strain microvariables generated by the theory. Once the stresses in each sub-cell are calculated, the overall stresses can be found as follows

$$\sigma_{ij} = \frac{1}{V} \sum_{\alpha,\beta,\gamma=1}^{2} V^{(\alpha,\beta,\gamma)} \sigma_{ij}^{(\alpha,\beta,\gamma)} \tag{3.5}$$

where V represents the total volume of the cell and $V^{(\alpha,\beta,\gamma)}$ the volume of a particular sub-cell.

3.2. Inelastic behaviour of metal matrix composites

A typical Metal Matrix Composites (MMC) comprises a fibre that behaves in an elastic manner up to the breaking stress and a matrix that will show the typical elastoplastic behaviour of a ductile material. To model a composite, an allowance must be made for the plastic deformation of the ductile matrix. In Aboudi's development of the theory of cells, he used the unified theory of plasticity developed by Bodner and Pardom. In this theory, plasticity is assumed to be always present throughout the loading process. Although rigorous, Bodner's *et al.* approach adds a level of complexity to the analysis that may not be necessary. In the present study, this has been abandoned in favour of a theory of plasticity proposed by Mendelson, in which the total strain experienced by a stressed material is made up of both elastic and plastic strains. Using this approach, plastic strain can be assumed to approximate to zero whilst the material is within the elastic region. This approach assumes simple elastic breakdown at the yield stress. For a biaxial loading system, the failure theory can be modified to include a shear yield component.

3.3. Randomly reinforced metal matrix composites and fatigue failure

The theory developed so far is for unidirectional short fibre and particulate composites where the fibres are aligned in the X_1 direction as shown in Fig. 2a. This places severe limitations on the type of systems possible to analyse. However, a transformation can be made on the stiffness matrix of each sub-cell, using a method first suggested by Arridge. It is found that for a material with randomly distributed fibres, the stiffness matrix reduces to three non-zero elements. Using this modified stiffness matrix in the stress strain matrix, the strain in all three dimensions can be calculated for each sub-cell in the MMC with randomly distributed fibres.

It can be assumed that fatigue failure will occur when one or more of the sub-cells reaches a critical stress level. In a one-dimensional loading system, the fatigue failure stress for the matrix material can be obtained from an S/N curve. It can be assumed that failure of the composite will occur for a similar number of cycles when any matrix sub-cell reaches this cyclic stress level provided the fibre has not reached its critical level. Therefore, the matrix is assumed to fail by fatigue similarly to the homogenous material.

The fibres however may behave differently. Silicon carbide fibres are brittle and do not exhibit fatigue failure. In the case of individual fibres, their critical fatigue stress is assumed to be identical to their tensile failure stress. However, similar fibres exhibit a wide range of tensile failure stresses, and this has important implications on the fatigue life of an MMC containing such brittle fibres

When the cyclic loading is high enough to break fibres, the outcome will be one of two possible behaviour patterns. First is that only a certain percentage of fibres break due to the fatigue loading, and the resulting redistribution of stresses ensures no more fibre breakage. In this event, the composite will eventually fracture by matrix fatigue failure. The second possibility is that as the fibres break the stress redistribution ensures more fibres will fail. Fatigue failure of the MMC is then by fibre failure.

3.4. Model of material cyclic plasticity

Technology of FE low-cycle fatigue simulation is based on the usage of a number of models: material cyclic behaviour model, concerned with one defect accumulation model and "died" element model describing LCF crack origin and evolution (Temis, 1989; Temis, 1994; Putchkov *et al.*, 1995; Fleming and Temis, 2002; Temis *et al.*, 2009). All of them are included in an original FE system for low-cycle fatigue simulation analysis. The theory of cyclic strain plasticity accompanied by the damage model based on the concepts of ultimate accumulated plasticity strain has been successfully employed for the prediction of fatigue lives in highly stressed Ti components (Putchkov *et al.*, 1995). Models of strain cyclic plasticity and strain-accumulated damage were employed to analyse behaviour and lifetime prediction of a plastic material with small rigid inclusions in the area of low cyclic fatigue (Fleming and Temis, 2002).

The branch of cycle strain curve at every halfcycle (Temis, 1989; Temis, 1994; Putchkov *et al.*, 1995) is defined on a basis of three-parametric model of material behaviour according to the accumulated plastic strain χ. This is defined as

$$\chi = \sum_{n=0}^{n_f} |\Delta\varepsilon_p| \tag{3.6}$$

The relationship between the stress σ_n^* and strain ε_n^* is represented in the form

$$\sigma^* = \begin{cases} E_\chi \varepsilon^* & \text{for} \quad \varepsilon^* \leqslant \varepsilon_{s\chi}^* \\ E_\chi \varepsilon_{s\chi}^* + b_\chi d_\chi \left[f\left(\varepsilon_S + \dfrac{\varepsilon^* - \varepsilon_{s\chi}^*}{b_\chi}\right) - \sigma_s \right] & \text{for} \quad \varepsilon^* > \varepsilon_{s\chi}^* \end{cases} \tag{3.7}$$

$$\varepsilon_{s\chi}^* = \frac{a_\chi}{d_\chi} \varepsilon_s \qquad d_\chi = \frac{E_\chi}{E}$$

where σ_s and ε_s are the initial stress and strain values at 0.02% offset yield; a_χ, b_χ and d_χ are material-sensitive parameters describing the plastic deformation response of the material under cyclic load; E_χ is a plastic strain path χ-dependant modulus such that $E = E_{\chi(\chi=0)}$. In practice, due to the Bauschinger effect, a_χ may be defined as $a_\chi = \sigma_{y\chi}/\sigma_s$, d_χ is defined as stated above and a transformation coefficient b_χ relates the non-linear portion of the stress–strain curve under monotonic loading to that observed under cyclic loading conditions.

This relationship is valid for the matrix material, which under cyclic load has an alternating elasto-plastic strain whilst the inclusion material remains elastic. Material constants describing the above mentioned parameters of cyclic stress-strain were defined on the base of experimental data obtained for the B95 Al alloy, whose parameters are equivalent to that of the Al7075 alloy. The aluminium alloy B95 under cyclic loading shows a decrease in the amplitude of plastic strain and the hardening effect with an increase in the number of cycles. It should be noted that Young's modulus of the Al alloy under cyclic loading decreases in the first cycles and recovers its value with increasing numbers of cycles. The main changes in the non-linear part of the Al alloy stress-strain curve take place in the first few half-cycles with maximum change taking place between the first and the third cycle. After the third cycle, the modulus slowly increases until the 100 th cycles, when the change in modulus ceases.

Tests conducted for different engineering materials showed that for constant-amplitude stress, constant-amplitude strain and stress random-amplitude loading, the number of half-cycles n_f before failure at alternating-sign plastic deformation is related to the limiting value χ_{max} by the power law

$$n_f = \left(\frac{\chi_{max}}{\delta}\right)^{\gamma} \tag{3.8}$$

here δ is the constant depending on the residual plastic strain value, γ is the parameter that characterises the material ability "to cure" the cyclic loading damage.

The model based on relationship (3.8) allows simulating the cyclic life exhaust process of the specimens under all conditions. If the value $D = \chi(n)/\chi_{max}(n)$ is taken as the measure of damage, $D = 1$ defines the amount of half-cycle loading where the alternating-sign plastic deformation takes place until a fatigue crack occurs. If, for different loading processes, the parameters defining the material mathematical model at cyclic deformation are equivalent to the same damage measure D, all functions of χ in (3.7) may be replaced by the functions of the dimensionless parameter D. The possibility of applying this approach has been studied experimentally (Putchkov and Temis, 1987; Temis and Putchkov, 1992). The values of parameters to be used in (3.7) were calculated on the base of experimental data from the results of constant strain controlled low-cycle fatigue studies that were conducted on un-notched specimens.

Once the value of D of a particular finite element reaches unity, the fatigue damage failure level of the material has been reached and $D = D_{limit}$. The elastic modulus E of the element will be reduced. The effect of this is that the contribution of the "died" element to the overall system stiffness will be sharply reduced and a redistribution of stress and strain to the neighbourhood elements will occur. Overall, some elements will experience a decrease in stress whilst others will be more highly stressed, and with the increasing number of cycles more "died" elements will occur causing further stress redistribution. At that it is possible to estimate a number of cycles to the crack origin from a condition of obtaining of failure rate to critical value D_{limit} and to retrace a crack evolution process that crack path is simulated the "died" elements (Temis *et al.*, 2009).

The cyclic elastoplastic material model based on the accumulated plastic strain concept is not the only possible. Another approaches are possible when different models based on strain energy estimation are applied for material behavior description. Review of these models is given in the paper by Macha (2001). Experimental researches carried out previously (Putchkov and Temis, 1987; Temis and Putchkov, 1992) were shown that accumulated plastic strain and plastic strain work under cyclic elastoplastic deformation bound by a linear relationship. This makes it possible to consider model (3.7) both in terms of the accumulated plastic strain and in terms of the plastic strain work under cyclic loading.

3.5. FE calculation procedure

Consider cyclic deformation under which the load vector $\mathbf{F}$ is applied to component by the following program

$$\mathbf{0} \to \mathbf{F}_{max} \to \mathbf{F}_{min} \to \mathbf{F}_{max} \to \cdots$$

If the strain and stress vectors in body points $\boldsymbol{\varepsilon}_k$ and $\boldsymbol{\sigma}_k$ correspond to the end of the k-th halfcycle of loading, and $\boldsymbol{\varepsilon}_{k+1}$ and $\boldsymbol{\sigma}_{k+1}$ correspond to the end of the $(k+1)$-th halfcycle, then for each halfcycle a variational relationship is carried out

$$\int_{\Omega} \boldsymbol{\sigma}_q^{\mathrm{T}} \delta\boldsymbol{\varepsilon}\, d\Omega - \int_{\Omega} (\mathbf{F}_{\Omega})_q^{\mathrm{T}} \delta\mathbf{u}\, d\Omega - \int_{S} (\mathbf{F}_s)_q \delta\mathbf{u}\, dS = 0 \tag{3.9}$$

where $q = k,\, k+1$ halfcycle number.

Subtracting from relation (3.9) at $q = k+1$ the similar one at $q = k$, one gets that a problem of the stress-strain condition simulation by change from the loading halfcycle to unloading one becomes a solution to the next problem

$$\int_{\Omega} (\Delta\boldsymbol{\sigma})^{\mathrm{T}}_{k+1}\delta\boldsymbol{\varepsilon}\, d\Omega - \int_{\Omega} (\Delta\mathbf{F}_{\Omega})^{T}_{k+1}\delta\mathbf{u}\, d\Omega - \int_{S_F} (\Delta\mathbf{F}_S)_{k+1}\delta\mathbf{u}\, dS = 0 \tag{3.10}$$

Having specified a relation form $\Delta\boldsymbol{\sigma}\,(\Delta\boldsymbol{\varepsilon})$, relation (3.10) by the well-known method (Temis and Putchkov, 1992) will become a finite element problem

$$\mathbf{K}_{k+1}\Delta\mathbf{U}_{k+1} = \Delta\mathbf{F}_{k+1} \tag{3.11}$$

where $\mathbf{K}_{k+1}$ is the stiffness matrix of the $(k+1)$-th halfcycle defined by a step-by-step approach; $\Delta\mathbf{U}_{k+1}$ and $\Delta\mathbf{F}_{k+1}$ are vectors of increments of the displacement and loading at halfcycle, correspondingly.

In that case, for the displacement vector at the $(k+1)$-th halfcycle, it is rightly

$$\mathbf{U}_{k+1} = \mathbf{U}_k + \delta\mathbf{U}_{k+1} \tag{3.12}$$

while the strain and stress in the calculated point are related by similar expressions

$$\boldsymbol{\varepsilon}_{k+1} = \boldsymbol{\varepsilon}_k + \Delta\boldsymbol{\varepsilon}_{k+1} \qquad \boldsymbol{\sigma}_{k+1} = \boldsymbol{\sigma}_k + \Delta\boldsymbol{\sigma}_{k+1} \tag{3.13}$$

Abstraction of the concept of a unified curve of strain is used. At the $(k+1)$-th halfcycle, a deformation process representing the point is to be on a branch of cycle strain curve (3.7) shown in Fig. 3 by the thick line outgoing from the point σ_k.
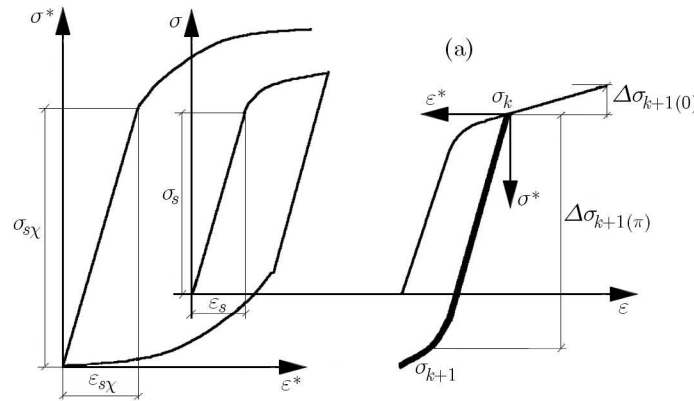
Fig. 3. Strain curve difinition for $(k+1)$-th halfcycle: (a) strain curve branches subject to loading direction

3.6. FE analytical model

In general, the stress-strain analysis of both the MMC and the individual cells within it are a $3D$ plasticity problem. However as a first approach (Fleming and Temis, 2002), the inclusions can be approximated to a spherical body surrounded by a cylinder of the matrix material as shown in Fig. 4a. The cylinder represents one cell of the MMC. The cylinder dimensions were defined by the condition that they were inscribed in the parallelepiped with height H and the base side $2R$, and all calculations were conducted for the model using $H = 2R$, where $R = 20\,\mathrm{mm}$ with the strain being in the direction of the cylinder axis, and was equal to the strain in the specimen. The strains in the transverse directions were equal to $-\nu_{MMC}\varepsilon_y$, where ν_{MMC} is Poisson's ratio of the MMC. In the elastic region, when $\varepsilon_y < 0.008$, a value of $\nu_{MMC} = 0.324$

was used, which was identical to the calculations carried out using the theory of cells. However, in the plastic region, Poisson's ratio must be continuously calculated as its value varies with increasing strain. For the first approach, we shall calculate ν_{MMC} on the base of the volume mixed model

$$\nu_{MMC} = \frac{\nu_{Al(elast)}\varepsilon_e + 0.5\varepsilon_p}{\varepsilon_y}0.88 + v_{SiC}0.12 \qquad (3.14)$$

Here ε_e is the elastic part of the matrix material strain, ε_p is the plastic part of the material strain, and $\varepsilon_y = \varepsilon_e + \varepsilon_p$.
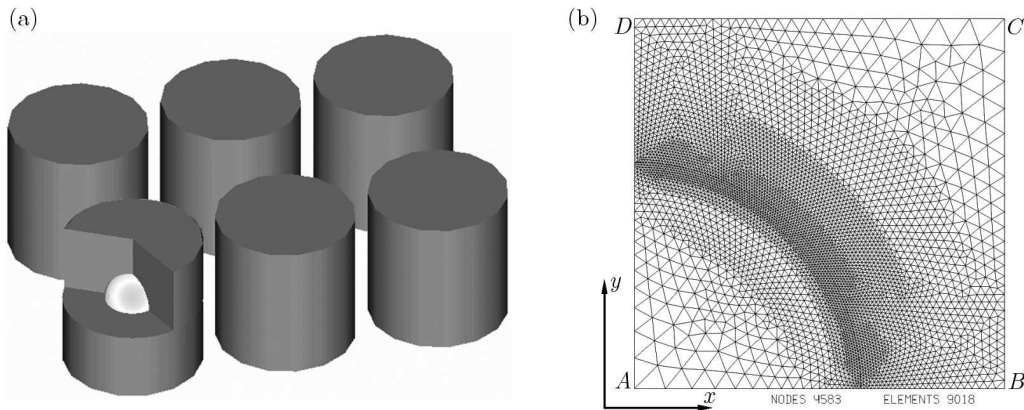

Fig. 4. (a) Schematic model of the MMC structure with a periodic array of fibres; (b) finite element mesh for the MMC with aspherical fibre

When considering the behaviour of the MMC under monotonic loading, a FE model with spherical inclusions containing 4583 nodal points each has two DOFs and 9018 axisymmetric simplex finite elements was used, as shown in Fig. 4b. When cyclic deformation was analysed, the meshes needed to be refined to decrease approximation errors and to increase the stability of FE models during various steps of mathematical simulation, whilst analysing an MMC with spherical inclusions, the number of nodes in the FE model during cyclic plasticity analysis was above 7000.

On the boundary AD, displacements in the x (radial) direction were fixed whilst displacements on the boundary AB were fixed in the y (cylinders axial) direction. On the boundary DC, displacements $\nu = \varepsilon_y R$ in the y direction were given. Corresponding displacements $u = -\nu_{MMC}\varepsilon_y R$ were given in the x direction on the boundary BC.

4. Results

Using the data experimentally obtained on the monolithic material, it was possible to predict the fatigue life of the MMC using the Theory of Cells and FE simulation.

The numerical investigation of the composite was carried out in strain-controlled tests for the following strain amplitudes of symmetric cycles, $\Delta\varepsilon_{ay} = 0.5\%, 0.6\%, 0.7\%, 0.8\%, 0.9\%, 1\%$. As for static loading simulation, it was assumed in the analysis that the inclusions in the composite were spherical. At each calculation point, the current values of χ and damage measure D were defined.

Figure 8 represents the accumulated plastic strain distribution after the fifth deforming half-cycles with an elongation amplitude of 1%. I denotes the concentration zone of accumulated plastic strain on the interface between the fiber and matrix. F denotes the concentration zone in the direction of load action.

The calculation process is stopped when $D = 1$ and an S/N diagram was plotted. The TOC prediction, FE calculation up to $D = 1$ and experimental results have been plotted as an S/N curve, and this is shown on Fig. 6.
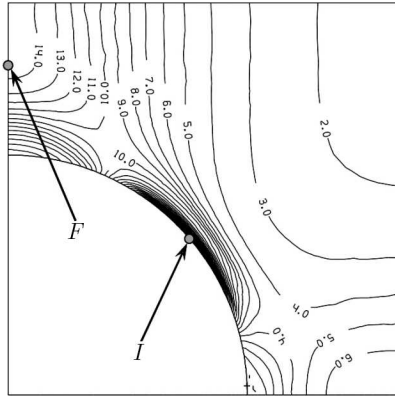

Fig. 5. Distribution of the accumulated plastic strain in the composite after 5 half-cycles with the elongation amplitude of 1%
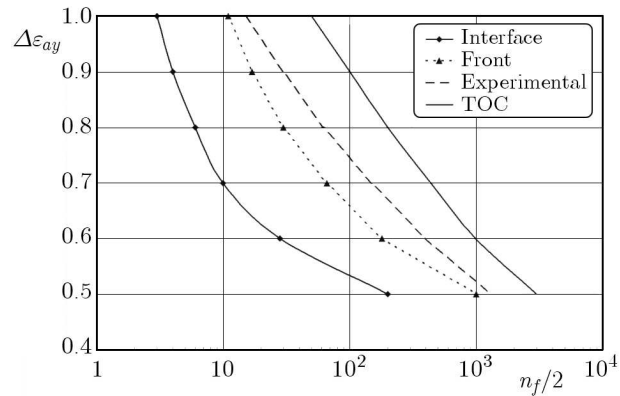

Fig. 6. Constant strain against cycles to failure. Experimental results and numerically predicted life by TOC and FE calculation of MMC Al7075+12% SiC

Cthe clculation results with using the "died" elements technique are shown in Fig. 7. LCF crack initiation is occurred at the interface zone point (Fig. 7a), then the crack grows from the interface, initiates at the frontal zone (Fig. 7b), the interface and frontal cracks merge (Fig. 7c), the crack initiates at the middle zone (Fig. 7d), interface-frontal and middle cracks merge (Fig. 7e). At last the crack exits to the outside of the specimen and full fracture of the material is occurred (Fig. 7f). This FE calculation up to full fracture with TOC prediction and experimental results have been plotted as an S/N curve, and this is shown in Fig. 8.
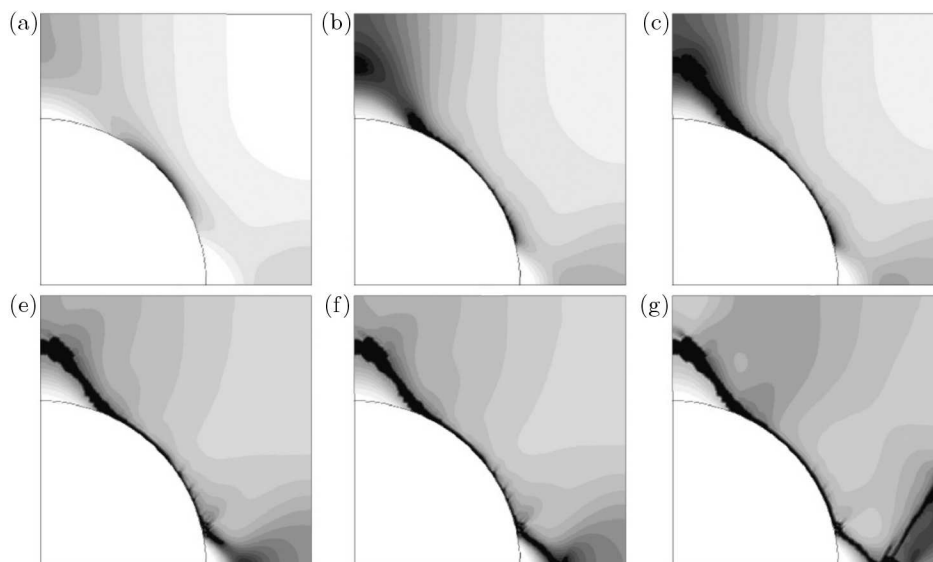

Fig. 7. LCF crack growth: (a) crack initiation at the interface zone point; (b) interface crack growth and crack initiation at the frontal zone; (c) interface and frontal crack merging; (d) crack initiation at the middle zone; (e) interface-frontal and middle cracks merging; (f) exit of the crack to the outside and full fracture of the material
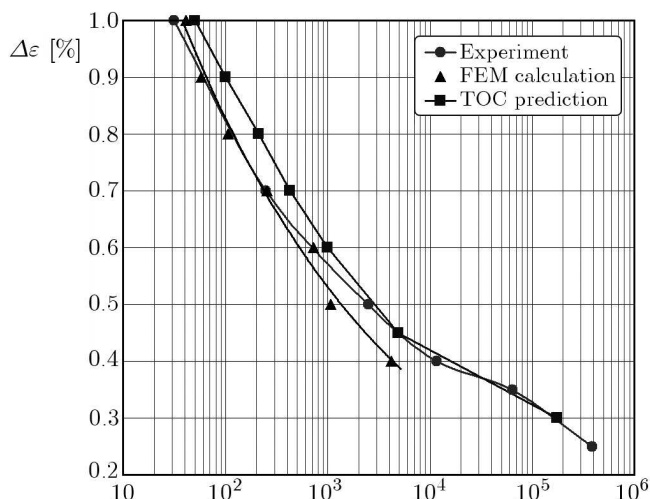
Fig. 8. Fatigue diagram up to full fracture

5.   Discussion

In Fig. 8, which gives results for the numerical investigation during fatigue loading it can easily be seen that two zones (I and F) appear where the accumulated plastic strain is at the maximum. The first zone I, is on the interface between the inclusion and matrix. The second zone F is formed at some distance from the inclusion in the direction of deformation, on the cylinder axis. This would indicate that the first fatigue crack forms on the inclusion matrix interface, but it is soon followed by the second crack that forms in the frontal zone after a certain number of loading and unloading half-cycles. Obviously, these cracks precede the overall MMC's failure. As long as some region of the composite is at high enough stress, this process will occur at all other levels of strain amplitude.

In the zones marked I and F in Fig. 5, the process of alternating-sign deformation occurs in different ways. Despite the fact that the overall loading process occurs at a constant strain amplitude, the zones I and F see a different stress and strain range. It should be noted that the process of cyclic elasto-plastic deformation brings an essential non-homogeneity in the distribution of plastic strain in the region close to the inclusion matrix interface. Due to the non-uniformity of hardening of aluminium in the region near the interface, a zone with wave-like distribution of plastic strain arises. However, with the number of half-cycles increasing, such a wave-like pattern is smoothed out. On the basic assumption that the number of half-cycles before the appearance of a low-cycle fatigue crack is defined by the condition $D = 1$, the number of cycles for crack initiation were calculated. It must be remembered that this finite element analysis only allows prediction of the number of cycles to crack initiation. For this type of fatigue loading, it would be expected that the number of cycles from the first crack until failure lies around 50-80% of the specimen cyclic lifetime. It should be expected therefore that, for a given strain level, theoretical predictions would under-estimate the life of the material compared to results obtained experimentally, and it can be seen from Fig. 6 that this is the case.

The TOC analysis was carried out over a larger number of cycles to failure. The numerical analysis and the results given in Fig. 6 show good agreement between the TOC prediction and the experimental results at the higher number of cycles. At strain levels below 0.007, the agreement is well within the experimental error of the test. However, once stresses are in the plastic region of the MMC, the prediction value of fatigue failure starts to deviate from the experimental results. At these levels, the stress in the particulates is significantly higher than that experienced in any sub-cell of the matrix. The matrix accommodates the increase in overall loading on the MMC

by yielding, but the particulates are still deforming elastically. As the load increases, some of the weaker particulates fail and there is a redistribution of the load between the particulate and matrix. The theory predicts that, for this MMC, the stress level in the individual particulates falls causing a corresponding increase in the stress on the matrix. So thefailure throughout the test should have been by matrix fatigue failure. A comparison of both the numerical method and the Theory of Cells is given in Fig. 6 and as can be seen the TOC overestimates the fatigue life of the composite whilst the numerical method using results obtained for the frontal zone underestimate the fatigue life. Further work is being carried out on both these methods to give a more accurate estimate of the fatigue life of metal matrix composites.

6. Conclusion

- Using fatigue data obtained from the matrix material and information on the failure stress of the particulate, it was possible to make a prediction of the fatigue life of a metal matrix composite material using both the Theory of Cells and a numerical method.

- The predicted fatigue life of the MMC using the method of cells was in close agreement with the experimental results for life outside the low cycle fatigue regime of 1000 cycles or less.

- Both the numerical method and the theory of cells can be used to predict fatigue life of a metal matrix composite within an acceptable degree of accuracy.

- A procedure for mathematical simulation of the elastoplastic deformation processes in a composite material including the metal base with short rigid inclusions under cyclic loading is presented. The results obtained show that the failure of the composite material occurs in several steps. The presented results of prediction of time of the composite material full fracture under cyclic loading are in well comparison with experimental data.

References

1. ABOUDI J., 1991, *Mechanics of Composite Materials – A Unified Micromechanical Approach*, Elsevier, Amsterdam, pp. 328

2. BATHEE K.-J., 1996, *Finite Element Procedures*, New Jersey, Prentice Hall, Inc., pp. 1038

3. FLEMING W.J., DOWSON A.L., 1999, Prediction of the fatigue life of an aluminium metal matrix composite using theory of cells, *Science and Engineering of Composite Materials*, **8**, 4, 181-189

4. FLEMING W.J., TEMIS J.M., 2002, Numerical simulation of cyclic plasticity and damage of an aluminium metal matrix composite with particulate SiC inclusions, *International Journal of Fatigue*, **24**, 1079-1088

5. MACHA E., 2001, A review of energy-based multiaxial fatigue failure criteria, *The Archive of Mechanical Engineering*, **XLVIII**, 71-101

6. PUTCHKOV I.V., TEMIS J.M., 1987, Elastoplastic and damage model of structure material, *Fifth USSR Symposium of Low Cycle Fatigue – Failure Criteria and Material Structures*, Volgograd, **2**, 50-52 [in Russian]

7. PUTCHKOV I.V., TEMIS Y.M., DOWSON A.L., DAMRI D., 1995, Development of a finite element based strain accumulation model for the prediction of fatigue lives in highly stressed Ti components, *International Journal of Fatigue*, **17**, 6, 385-398

8. TEMIS J.M., 1989, Plasticity and creep of GTE components under cyclic loadings, *Problems of Strength and Dynamics of Aviation Motors, Vol. 4, CIAM Proceedings*, **1237**, 32-50 [in Russian]

9. TEMIS J.M., 1994, Simulation of processes of non-isothermal elastoplastic deformation energy power plant components, [In:] *Dynamics and Strength of Machines. Mechanism and Machine Theory*, K.V. Frolov et al. (Edit.), Vol. 1-3, Moscow, Mashinostroenie, 263-268 [in Russian]

10. TEMIS Y.M., AZMETOV KH.KH., ZUZINA V.M., 2009, Low-cycle fatigue simulation and lifetime prediction of high stressed structures, *Solid State Phenomena, Trans. Techn. Publications*, Switzerland, **147-149**, 333-338

11. TEMIS J.M., PUTCHKOV I.V., 1992, Characteristics of elastoplastic deformation and failure rate of structure materials under cyclic loading, [In:] *Articles "Applied Problems of Durability and Plasticity. Solution methods"*, Nizhny Novgorod University, 82-89 [in Russian]

Porównanie dwóch modeli symulacji numerycznej niskocyklowego zmęczenia materiału plastycznego z drobnymi i sztywnymi wtrąceniami

Streszczenie

W pracy zastosowano teorię komórkową i numeryczną metodę elementów skończonych opartą na odkształceniowo cyklicznej plastyczności, wprowadzono model zniszczenia oraz uwzględniono technologię wytłaczania do określenia trwałości zmęczeniowej kompozytów metalowo-ceramicznych. Wyniki obliczeń porównano z badaniami doświadczalnymi. Zaobserwowano, że wyniki teoretyczne uzyskane z zastosowaniem teorii komórkowej były w zgodzie z eksperymentem dla niskocyklowego obciążenia zmęczeniowego, tj. dla 1000 cykli i poniżej. Rezultaty otrzymane w drodze symulacji numerycznych modelu matematycznego wskazały, że zniszczenie zmęczeniowe przebiega w kilku etapach – w wyniku akumulacji uszkodzeń i wskutek wzrostu szczeliny. Obliczenia czasu do pełnego pęknięcia kompozytu pokryły się z wynikami doświadczalnymi w dobrym stopniu. Po porównaniu efektywności metody numerycznej oraz teorii komórkowej stwierdzono w podsumowaniu, że obydwie metody mogą być stosowane do wyznaczania trwałości zmęczeniowej metalowo-ceramicznych materiałów kompozytowych z uzyskaniem zadawalającej dokładności.